Fish and Shellfish Immunology 93 (2019) 161–173

Contents lists available at ScienceDirect

Fish and Shellfish Immunology

journal homepage: www.elsevier.com/locate/fsi

Full length article

Subfunctionalization and evolution of liver-expressed antimicrobial peptide 2 (LEAP2) isoform genes in Siberian sturgeon (*Acipenser baerii*), a primitive chondrostean fish species

Chan-Hee Kim[1], Eun Jeong Kim[1], Yoon Kwon Nam[*]

Department of Marine Bio-Materials & Aquaculture, Pukyong National University, Busan, 48513, South Korea

ARTICLE INFO

Keywords:
Siberian sturgeon *Acipenser baerii*
LEAP2 isoforms
Evolution
Isoform subfunctionalization

ABSTRACT

Two liver-expressed antimicrobial peptide 2 (LEAP2) isoforms were characterized in a primitive chondrostean sturgeon species, *Acipenser baerii* (Acipenseriformes). *A. baerii* LEAP2 isoforms represented essentially common structures shared by their vertebrate orthologs at both genomic (*i.e.,* tripartite organization) and peptide (two conserved disulfide bonds) levels. *A. baerii* LEAP2 isoforms (designed LEAP2AB and LEAP2C, respectively) phylogenetically occupy the most basal position in the actinopterygian lineage and represent an intermediate character between teleostean and tetrapodian LEAP2s in the sequence alignment. Molecular phylogenetic analysis including LEAP2s from extant primitive fish species indicated that the evolutionary origin of ancestral LEAP2 in vertebrate groups should date back to earlier than the actinopterygian-sarcopterygian split. Gene expression assays under both basal and stimulated conditions suggested that *A. baerii* LEAP2 isoforms have undergone substantial subfunctionalization in tissue distribution pattern, developmental/ontogenetic expression, and immune responses. LEAP2AB showed a predominant liver expression, while LEAP2C exhibited the highest level of expression in the intestine. LEAP2C was a more dominantly expressed isoform during embryonic development and prelarval ontogeny. The LEAP2AB isoform is more closely associated with innate immune response to microbial invasion, compared with LEAP2C, as evidenced by results from LPS, poly(I:C) and *Aeromonas hydrophila* challenges. Synthetic mature peptides of LEAP2AB displayed a more potent antimicrobial activity than did LEAP2C. Data from this study could be useful not only to provide deeper insights into the evolutionary mechanism of LEAP2 in the actinopterygian lineage but also to better understand the innate immunity of this commercially important chondrostean species.

1. Introduction

Sturgeons (Acipenseriformes) represent an ancient lineage of Actinopterygii (ray-finned fishes), often referred to as living fossils [1]. Phylogenetically, sturgeons belong to a chondrostean fish group that occupies an evolutionary bridge between Chondrichthyes (cartilaginous fish) and Osteichthyes (bony fish). Given their unique phylogenetic position, sturgeons are recognized as an invaluable comparative model for studying evolution and diversifying mechanisms of many biological systems in the vertebrate lineage [2–4]. In addition to their theoretical and evolutionary relevance, sturgeons have been long recognized as valued fishery resources primarily as a source of caviar. However, most natural stocks of all the acipenseriform species have been endangered or threatened due to multiple anthropogenic and industrial activities, and aquacultural production has already become a mandatory means to utilize sturgeon and its products for commercial purposes worldwide [5]. As aquaculture of sturgeons has increased considerably over the past decades, a parallel increase in risk associated with infectious diseases has occurred under intensive farming conditions [6,7]. In recent years, bacterial and viral pathogens have been identified as causing high mortality outbreaks in farmed sturgeon stocks, suggesting an urgent need for disease control [8–10]. In this context, the preparation of a catalogue of genes related to immunity would be an essential component in understanding the ability of sturgeons to mount specific immune response(s) to pathogen invasion [11–15].

Liver-expressed antimicrobial peptide 2 (LEAP2) is the second blood-derived antimicrobial peptide (AMP), which was first isolated in humans [16]. As a member of the cationic AMP family, LEAP2 is

[*] Corresponding author. Department of Bio-Materials and Aquaculture, College of Fisheries Sciences, Pukyong National University, 45 Yongso-ro, Nam-gu, Busan, 48513, South Korea.
E-mail address: yoonknam@pknu.ac.kr (Y.K. Nam).
[1] These two authors contributed equally to this study.

https://doi.org/10.1016/j.fsi.2019.07.040
Received 3 December 2018; Received in revised form 8 July 2019; Accepted 14 July 2019
Available online 15 July 2019
1050-4648/

considered a vital component of the innate immune system against microbial invasion and is also known to act a modulator of other immune factors [17–20]. In fish external fertilization and development, the involvement of LEAP2 in the protection of embryos and early larvae from microbial invasion has also been proposed [21,22]. To date, genetic determinants of LEAP2 have been identified in various fish species belonging to a wide array of taxonomic positions (mostly teleosts). Previous studies on fish LEAP2 peptides have indicated that most teleosts possess at least two paralogue LEAP2 isoforms and that teleostean members share a conserved structural similarity of LEAP2 at both genomic (*i.e.,* tripartite exon-intron organization) and protein (*i.e.,* core structure with two disulfide bonds in mature peptides) levels [23–25]. However, in spite of their structural homology, transcriptional regulation of teleostean LEAP2s under both non-stimulated and immune-challenged conditions is largely variable depending on species, isoforms, and stimuli, suggesting potential diversification and subfunctionalization of LEAP2 isoforms in a species and lineage-specific fashion [22,23,25,26].

In contrast to the large body of information regarding teleostean LEAP2s, relatively little LEAP2 data are available for the chondrostean fish group. A recent study reported LEAP2 isoforms from two *Acipenser* species (*A. dabryanus* and *A. sinensis*) with proposed contributions of LEAP2 to innate immunity in this fish group, and indicated that chondrostean LEAP2s also shared conserved structures with other vertebrate orthologs [27]. However, the evolutionary relationship of chondrostean LEAP2s in the vertebrate lineage has not been adequately addressed, and more importantly, their expression characteristics and antimicrobial activities have remained largely unexplored. From that previous study, expression of one LEAP2 isoform in certain sturgeon species (as exemplified by LEAP2B in *A. dabryanus*) could be extremely low or even undetectable, suggesting that isoform-specific regulation of LEAP2 genes might have been diversified among *Acipenser* species, and thus should be further investigated in other sturgeon species [27]. Thus, little is known regarding isoform-specific or isoform-dependent roles of chondrostean LEAP2s.

Accordingly, the objective of this study was to characterize two functional LEAP2 isoforms from the Siberian sturgeon (*Acipenser baerii*), a popularly aquacultured *Acipenser* species in many countries, including South Korea [28]. We revisited the phylogenetic relationships of these chondrostean LEAP2s in the vertebrate lineage to hypothesize more fully the origin and evolution of LEAP2 isoforms. To examine the potential subfunctionalization between chondrostean LEAP2 isoforms, we performed various expression assays with regard to basal expression patterns (tissue expression, developmental modulation, and ontogenetic regulation) and transcriptional responses to different stimulatory treatments including lipopolysaccharide (LPS), polyinosinic:polycytidylic acid [poly(I:C)], and *Aeromonas hydrophila* challenge. Also we compared antimicrobial activities of synthetic LEAP2AB and LEAP2C mature peptides against certain gram (+) and gram (−) bacteria.

2. Materials and methods

2.1. Fish specimens and ethics statement

Siberian sturgeon *A. baerii* specimens used in this study were laboratory stock that had been artificially propagated and reared in the Experimental Fish Culture Station, Pukyong National University, Busan, South Korea. Fish were maintained with a water recirculating system at 18-20 °C and fed with a commercial diet (Millennium plus; Woosung feed Co., Daejeon, Korea) with a daily feeding rate of 0.8–1% of body weight. Our experiments were approved by the Animal Care and Use Committee of Pukyong National University (Approval number 201818). All experimental procedures were performed in accordance with the National Act on Laboratory Animals.

2.2. Molecular cloning of A. baerii LEAP2 cDNA and genomic isoforms

Partial next-generation sequencing (NGS) clones representing LEAP2-like sequences were obtained from our local NGS transcriptome database built with *A. baerii* liver (data not shown). Based on alignment with *Acipenser* orthologs available in GenBank (NCBI), oligonucleotide primers were designed for rapid amplification of cDNA ends (RACE) at both 5′- and 3′ -directions using a FirstChoice RLM-RACE kit (Thermo Fisher Scientific, Waltham, MA USA) and liver total RNA. Oligonucleotide primers used in this study were listed in Suppl. Table S1. Based on the contig assembly of putative cDNA sequences for each LEAP2 isoform, a continuous version of full-length cDNA for each isoform was isolated from the liver total RNA using reverse transcription PCR (RT-PCR). RT-PCR products were cloned into a pGEM-T-easy vector (Promega, Madison, WI, USA) and sequenced (six clones per isoform) at both directions by primer walking. Based on the cDNA sequences, a genomic gene segment of each LEAP2 isoform was amplified from fin genomic DNA purified from a female *A. baerii* using a pair of PCR primers complementary to the 5′- and 3′-untranslated regions (UTR), respectively. PCR products were TA cloned and sequenced ($n = 4$ for each isoform) as described previously. Exon-intron organization of the putative genomic gene of each isoform was determined based on the comparison with its cDNA counterpart.

2.3. Bioinformatic sequence characterization and molecular phylogeny

The amino acid sequence of each LEAP2 isoform was deduced from its cDNA sequence using the open reading frame (ORF) finder (https://www.ncbi.nlm.nih.gov/orffinder/). Putative cleavage sites for a signal peptide and a mature peptide in the deduced sequences were predicted using SignalP 4.1 (http://www.cbs.dtu.dk/services/SignalP/) and the ProP 1.0 server (http://www.cbs.dtu.dk/services/ProP/). Theoretical isoelectric point (*p*I) values of peptides/proteins were calculated using the ExPASy Compute pI/Mw tool (https://web.expasy.org/compute_pi/). Multiple sequence alignments of *A. baerii* LEAP2 isoforms with vertebrate orthologs were conducted using ClustalW (https://www.genome.jp/tools-bin/clustalw) and refined manually. Molecular phylogenetic trees were reconstructed using maximum likelihood (ML) and neighbor-joining (NJ) methods using MEGA software (ver. 10.0.5; https://www.megasoftware.net/). For both trees, the Jones-Taylor-Thornton (JTT) model was used as a substitution model. Gaps were treated as partial deletions with a site coverage cutoff of 25%. The confidence of tree topology was tested with 1000 bootstrap replicates. Sequences used for multiple sequence alignments and molecular phylogeny are provided in Suppl. Table S2.

2.4. Tissue distribution assay

To examine the tissue distribution pattern and basal expression levels of LEAP2 isoform mRNAs under non-stimulated conditions, ten tissues, including the brain, eye, fin (caudal fin), gill, heart, intestine (mid-intestine), kidney, liver, muscle (dorsal muscle), and spleen were surgically obtained from twelve healthy individuals [5-month-old, average body weight (BW) = 20.6 ± 3.1 g and total length (TL) = 21.2 ± 2.5 cm]. Tissues were immediately frozen on dry ice and stored at −85 °C until used. Equal amounts of tissue (20 mg) from four individuals were pooled within a given tissue type to prepare three replicate batches.

2.5. Developmental and ontogenetic expression assay

To examine the expression patterns of LEAP2 isoforms in developing embryos and prelarvae, induced spawning was performed using luteinizing hormone-releasing hormone analog (LHRHa; Sigma-Aldrich, St. Louis, MO, USA) as described previously [28]. Eggs obtained from two females (average BW = 21.5 ± 2.1 kg) were pooled (approximately

33,000 eggs from each female) and inseminated with pooled sperm from three males (average BW = 16.5 ± 2.9 kg). Upon fertilization, embryos were incubated at 20 ± 0.5 °C until hatching, and 12 developmental samples (approximately 110 embryos at each stage) were obtained in triplicates at just fertilized (JF; 0 h post insemination; HPI), first cleavage (FC; 2 HPI), eight cells (8C; 3.5 HPI), early blastula (EB; 9.6 HPI), onset of gastrulation (OG; 20 HPI), small yolk plug formation (SYP; 28 HPI), onset of neurulation (ON; 33 HPI), elongation of excretory rudiment (EER; 37 HPI), heart rudiment, and tail budding (HR; 59 HPI), S-heart formation (SH; 73 HPI), tail-end reaching the head (TRH; 101 HPI), and first hatching (FH; 119 HPI). Embryological characteristics of each stage were referenced to our previous work [28]. After hatching, prelarvae (≒ 36 prelarvae) were sampled in triplicates at 1, 3, 5, 7, 9, and 11 days after hatching (DAH) from the prelarval nursery tanks at 20 °C. Morphological development and size of the prelarvae were referenced from a previous description [29]. Embryo and prelarval samples were frozen on dry ice.

2.6. LPS and poly(I:C) challenges

To examine the transcriptional responses to immune-stimulatory LPS treatment, *A. baerii* individuals (average BW = 19.4 ± 2.1 g; $n = 6$) were administered an intraperitoneal (IP) injection of LPS (*Escherichia coli* 0111: B4, Sigma-Aldrich, USA) at doses of 10, 50, and 100 μg/g BW. LPS was resuspended in phosphate buffered saline (PBS, pH 7.4) and the injection volume was 200 μL. A non-challenged control group ($n = 6$) was prepared by an injection of an equal volume of PBS. After injection, fish were assigned to one of four tanks containing 300 L of 1 μm-filtered groundwater at 20 °C. At 24 h post-injection (HPI), four individuals were randomly chosen from each group, and tissues (liver, kidney, and spleen) were surgically obtained individually for gene expression assays. Conversely, for poly(I:C) challenge, fish ($n = 6$) were intraperitoneally injected with poly(I:C) (Sigma-Aldrich, USA) at doses of 20 and 100 μg/g BW. The unchallenged control group ($n = 6$) was also administered an IP injection of the same volume (200 μL) of PBS. Post-injection handling, including tissue sampling at 24 HPI, was similar to that described for the LPS challenge above. Based on the expression data at 24 HPI, tissue showing the greatest expression modulation of LEAP2 isoforms in response to either LPS or poly(I:C) challenge was selected and further subjected to analysis of time course expression patterns of LEAP2 isoforms. Expression levels of LEAP2AB and LEAP2C isoforms were compared in the kidney for their modulations in response to LPS injection (100 μg/g BW), while in the spleen in response to poly(I:C) challenge (100 μg/g BW). Four randomly chosen individuals were sampled at 12, 18, 24 and 48 HPI. All other experimental conditions including the preparation of PBS-control group and tank conditions were the same with those described above.

2.7. Bacterial challenge

A bacterial challenge experiment was performed with *Aeromonas hydrophila* KCTC 2358. Freshly grown bacteria were washed twice with sterile PBS and resuspended in PBS. *A. baerii* individuals ($n = 24$; average BW = 24.1 ± 3.9 g) were administered an IP injection of the bacterial suspension (200 μL) at doses of 2×10^8 cfu/g BW. Based on our preliminary study, the bacterial concentration used in this study corresponds to one very close to the maximum sublethal dose (almost all viable until 1 week after IP injection) for *A. baerii* juveniles described above. Injected fish were assigned to one of two replicate 300-L tanks at 20 °C (*i.e.,* 12 fish per tank). An unchallenged control group was also prepared with PBS injection and also assigned into two same-sized tanks. After injection, two individuals were randomly chosen from each tank (*i.e.,* $n = 4$ each from the *A. hydrophila*-injected and PBS-injected groups) at 6, 12, 18, 24, and 48 HPI. From each, the liver, kidney, and spleen tissues were surgically removed, frozen on dry ice, and stored at −85 °C until used.

2.8. RNA preparation and real-time reverse transcription PCR (RT-qPCR) assay

Total RNA was extracted with Trizol reagent (Thermo Fisher Scientific, USA) and purified with an RNeasy Plus Micro Kit (Qiagen, Hilden, Germany) including the DNA removal step. Integrity of total RNA was verified with 28S rRNA: 18S rRNA ratio (*i.e.,* band intensity of approximately 2: 1 determined with gel image analysis software installed in a Bio-Rad XR Gel documentation system; Bio-Rad, Hercules, CA, USA) in ethidium-bromide (EtBr)-stained MOPS/formaldehyde agarose gel (1%). The purity and concentration of total RNA were measured with a NanoDrop™ ND-1000 spectrophotometer (Thermo Fisher Scientific, USA). The ratios of both 260 nm/280 nm and 260 nm/230 nm were confirmed to be at least higher than 1.9. An aliquot (2 μg) of total RNA from each batch was reverse transcribed using an Omniscript Reverse Transcription Kit (Qiagen, Germany) according to the manufacturer's instructions. Synthesized cDNA samples were 10-fold diluted, and 2 μL of the diluted template was subjected to RT-qPCR amplification. An *A. baerii* 18S rRNA (AY904463.1) was also amplified from each cDNA sample as a normalization control for LEAP2 mRNA expression levels. PCR efficiency of each primer pair, including that for the 18S rRNA control, was at least higher than 0.93. RT-qPCR was carried out in triplicates using the LightCycler 480 Real-Time PCR System and LightCycler 480 SYBR Green I Master mix (Roche Applied Science, Penzberg, Germany). Relative expression of each LEAP2 isoform in each tissue (*i.e.,* tissue distribution assay) or developmental sample (*i.e.,* embryonic and ontogenetic expression assay) was estimated based on the normalization of LEAP2 expression levels against the 18S rRNA expression using the $2^{-\Delta CT}$ method [30,31]. In the differential expression assay during stimulatory challenges, expression levels of LEAP2 isoforms in challenged groups were expressed as fold-changes relative to that in the PBS-control group based on the normalization against 18S rRNA control using the $2^{-\Delta\Delta CT}$ method [30,31]. Differences in expression levels were assessed using ANOVA followed by Duncan's multiple range test and/or Student's *t*-test at the level of $P = 0.05$.

2.9. Antimicrobial activity assay of LEAP2AB and LEAP2C

The putative mature LEAP2AB and LEAP2C were commercially synthesized with over 95% purity (Anygen, Gwang-ju, South Korea), both of which contain the cysteine connectivity with Cys^{1st}-Cys^{3rd} and Cys^{2nd}-Cys^{4th}. The synthesized peptides were analyzed by high-performance liquid chromatography (Shimadzu HPLC Lab solution, Kyoto, Japan) and MALDI-TOF mass spectroscopy (AXIMA Assurance, Shimadzu, Japan) (Suppl. Fig. S1). The antimicrobial activities of the synthetic *A. baerii* LEAP2AB and LEAP2C were investigated using ultrasensitive radial diffusion assay (URDA) as described previously [15]. The synthetic peptides were dissolved in water, which was made to a concentration of 8, 4, and 2 μg/μL through two-fold serial dilution. An aliquot (5 μL) of each concentration was added to a well of underlay gel with 1 mm thick and 2.5 mm in diameter. Bacterial strains used in this study were gram-positive bacteria, including *Bacillus subtilis* KCTC 1021, *Staphylococcus aureus* KCTC 1621, *Streptococcus iniae* FD 5228, and gram-negative bacteria, including *A. hydrophila* KCTC 2358, *Escherichia coli* ML 35, and *Vibrio anguillarum* KCTC 2711.

3. Results

3.1. Characteristics of cDNA and deduced amino acid sequences

Two LEAP2 isoforms (LEAP2AB and LEAP2C designated in this study based on molecular phylogeny) were isolated from *A. baerii*. Complementary DNA of *A. baerii* LEAP2AB (GenBank accession number: MK246407) was comprised of a 95-bp 5′-untranslated region (UTR), a 288-bp open reading frame (ORF) including a TAA stop codon

encoding a precursor protein of 95 amino acids (aa), and 682-bp 3′-UTR excluding poly(A+) tail. In the 3′-UTR, three putative polyadenylation signals (AATAAA) were observed at 328 bp, 315 bp, and 13 bp prior to the poly(A+) tail. Conversely, *A. baerii* LEAP2C cDNA (MK246409) contained an ORF of 246 bp encoding an 81-aa precursor protein, a 5′-UTR of 38 bp, and a 3′-UTR of 593 bp. A putative polyadenylation signal with a canonical sequence (AATAAA) was predicted at 20 bp prior to the poly(A+) tail. The stop codon of *A. baerii* LEAP2C was TAG.

Calculated molecular weight of full-length *A. baerii* LEAP2AB polypeptide was 10.55 kDa, with a theoretical *p*I value of 9.08. The predicted mature peptide of *A. baerii* LEAP2AB (cleavage site between Arg^{54} and Met^{55}) was estimated to encode 41 aa (4.75 kDa; *p*I = 8.88). However, bioinformatics software did not clearly predict the cleavage site for the signal peptide in *A. baerii* LEAP2AB. Conversely, the molecular weight and *p*I value of the entire *A. baerii* LEAP2C polypeptide were estimated to be 9.27 kDa and 9.15, respectively. *A. baerii* LEAP2C exhibited a putative signal peptide cleavage site between Ala^{25} and Ala^{26} as well as a cleavage site for the mature peptide between Arg^{42} and Ser^{43}. The resulting mature peptide of *A. baerii* LEAP2C (39 aa) exhibited a molecular mass of 4.59 kDa with a theoretical *p*I value of 7.65. *A. baerii* LEAP2AB and AbLEAP2C exhibited low sequence identity with each other (22% out of 95 aligned positions) over the whole protein region, although the identity was slightly increased at mature peptide regions (32%) (Fig. 1).

3.2. Genomic organization

Each *A. baerii* LEAP2 isoform gene displayed a tripartite gene organization (three exons interrupted by two introns). The *A. baerii* LEAP2AB gene (MK246408) showed 69 bp of coding exon-1, 179 bp of exon-2, and 40 bp of exon-3 (including the stop codon), intervened by the 1580-bp intron-1 and 919-bp intron-2. Each exon coded 23, 60, and 12 aa. Coding regions of the genomic gene matched well with the sequence of its cDNA counterpart. The consensus GT-AG exon-intron boundary rule was conserved in intron-1; however, intron-2 showed G**C**-AG. In contrast, the *A. baerii* LEAP2C gene (MK246410) was represented by 66-bp exon-1 (22 aa encoded), 143-bp exon-2 (48 aa) and 37-bp exon-3 (11 aa). It had longer introns than LEAP2AB, especially for intron-2 (919 bp for LEAP2AB and 2714 bp for LEAP2C). A conserved GT-AG rule was consistent at every exon-intron junction site in LEAP2C (Fig. 1).

3.3. Multiple sequence alignments of mature peptide regions

Based on the multiple sequence alignments of *A. baerii* LEAP2 isoforms (mature peptide region) with its corresponding vertebrate orthologues, both *A. baerii* LEAP2AB and LEAP2C represented structural features typical of vertebrate LEAP2s, notably including the four conserved Cys residues, which are likely to form two intramolecular disulfide bonds. The RXXR motif in front of the N-terminus of the predicted mature peptide was also well-conserved in all LEAP2 isoform sequences aligned. In the alignment *A. baerii* LEAP2AB mature peptide sequences along with teleostean and tetrapodian orthologs, 13 residues out of 50 aligned positions were conserved among all the sequences aligned (43 putative neopterygian LEAP2As, three chondrostean LEAP2AB, eight known teleostean LEAP2Bs and nine tetrapodian LEAP2s) (Suppl. Fig. S2). The *A. baerii* LEAP2AB mature peptide exhibited the highest sequence identity to orthologs from other *Acipenser* species (97.8%), as expected. Among orthologs from neopterygian members, an isoform of LEAP2 from a holostean species (*Lepisosteus oculatus*) showed the highest sequence identity to *A. baerii* LEAP2AB (71.1%). When compared to orthologs from teleosts, the *A. baerii* LEAP2AB displayed the highest identity to the ortholog from an osteoglossiform species, *Scleropages formosus* (71.1%). In addition, *A. baerii* LEAP2AB exhibited relatively higher sequence identities to teleostean LEAP2As from Elopomorpha, Otomorpha, or Protacanthopterygii (all having 41-aa mature peptides; identity = 66.7–73.3%), than to those from Acanthopterygii, with 44- or 46-aa mature LEAP2A peptides (identity = 48.0–58.0%). Meanwhile, in a comparison between *A. baerii* LEAP2AB and teleostean LEAP2B, *A. baerii* LEAP2AB represented relatively higher sequence identity with protacanthopterygian LEAP2Bs (62.2–66.7%) than with ostariophysian LEAP2B orthologs (51.1–57.8%). Furthermore, the sequence identities between *A. baerii* LEAP2AB and tetrapodian LEAP2s ranged from 40.9% (with *Gallus gallus* and *Xenopus tropicalis*) to 45.5% (with *Pelodiscus sinensis*).

In the alignment of LEAP2Cs, three *Acipenser* species shared an identical mature peptide sequence (Fig. 2). In comparison with orthologs from other primitive species, *A. baerii* LEAP2C showed the highest sequence identities to orthologs from *L. oculatus* (74.4%) and *S. formosus* (69.8%). *A. baerii* LEAP2C displayed different identities to two isoforms from a chimaeriform species (*Callorhinchus milii*; Holocephali; Chondrichthyes): 52.3% sequence identity with *C. milii-1* while 59.6% with *C. milii-2*. Meanwhile, *A. baerii* LEAP2C shared 57.8% identity with a coelacanthiform ortholog from *Latimeria chalumnae* (Sarcopterygii). When compared with teleostean LEAP2Cs, *A. baerii* LEAP2C represented moderate sequence identities to protacanthopterygian LEAP2Cs (58.1–60.5%) and acanthopterygian and ostariophysian LEAP2Cs orthologs (46.5–55.8%). *A. baerii* LEAP2C showed sequence identities of less than 50% to tetrapodian orthologs.

Sturgeon LEAP2s (especially the LEAP2C isoform) displayed several

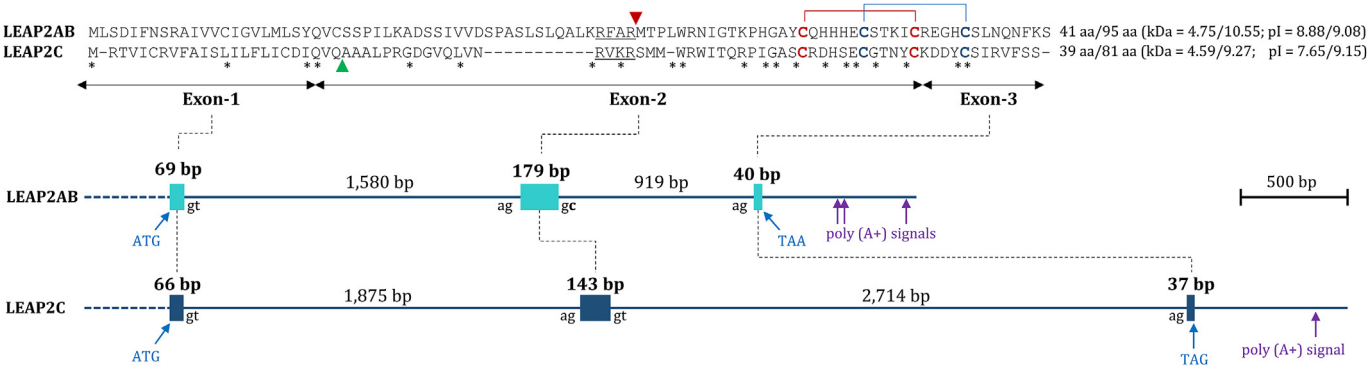

Fig. 1. Primary polypeptide structures of *Acipenser baerii* LEAP2AB and LEAP2C isoforms (*upper*) and their genomic exon-intron organization patterns (*lower*). In pairwise alignment, the RXXR cleavage motif for mature peptides is underlined and the cleavage site is indicated by a red arrowhead. For LEAP2C, the predicted cleavage site for the signal peptide is noted by a green arrowhead. Conserved cysteine residues likely to form two disulfide bonds are lined. In the schematic drawing of the tripartite exon-intron organization of each isoform, an ATG translation initiation codon, a stop codon, and polyadenylation signals are noted. The LEAP2AB gene has a noncanonical GC-AG boundary sequence in its intron-2. (For interpretation of the references to colour in this figure legend, the reader is referred to the Web version of this article.)

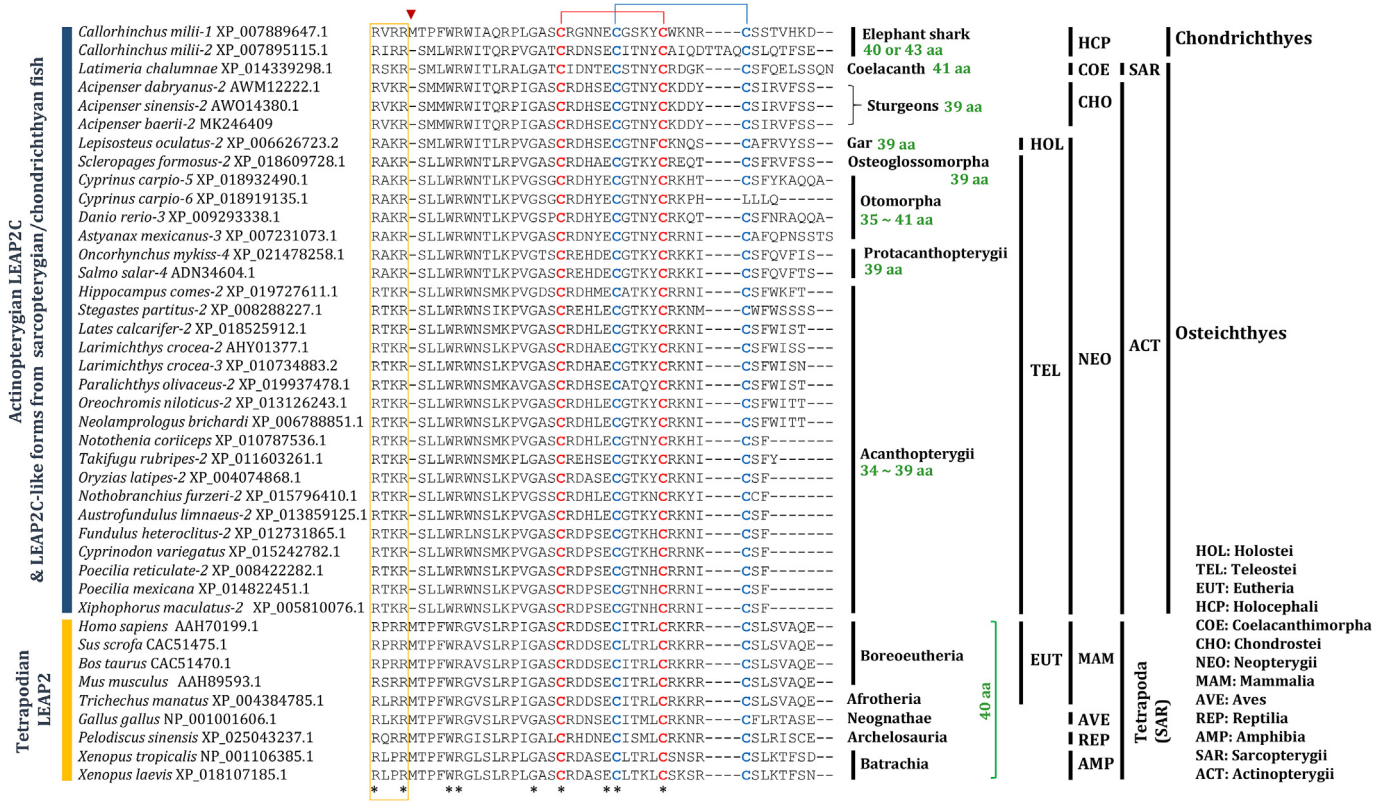

Fig. 2. Multiple sequence alignments of chondrostean LEAP2C isoforms along with their actinopterygian and tetrapodian orthologs. The RXXR cleavage motif for the mature peptide is boxed, and the cleavage site is indicated by an arrowhead on the top. Conserved cysteine residues likely to form two disulfide bonds are lined.

amino acid residues shared by either teleostean or tetrapodian orthologs. For example, in LEAP2C alignment, the Lys[3] (aligned position) in the RXXR motif and Ser[6] in chondrostean LEAP2Cs were shared by all other actinopterygian orthologs, whereas tetrapods (except *Gallus gallus*) exhibited Arg[3] and Thr[6], respectively. Conversely, chondrosteans together with other ancient primitive species showed an Arg[15] that was also conserved in tetrapodian LEAP2Cs, whereas all other teleostean (except *S. formosus*) LEAP2Cs exhibited a Lys[15] at that position. Meanwhile, the two LEAP2 isoforms from a chimaeriform species, *C. milii* (Holocephali; Chondrichthyes) showed considerably different sequence structures. The *C. milii-1* isoform more closely resembles tetrapodian LEAP2s, particularly at their N-terminal regions (*i.e.,* an exactly matched Met-Thr-Pro-Phe sequence), whereas *C. milii-2* exhibited greater resemblance to actinopterygian LEAP2Cs at the N-terminal region. Notably, *C. milii-2* possess four additional amino acids in the 3rd loop (*i.e.,* between 3rd Cys and 4th Cys residues). LEAP2 sequences predicted in a lobe-finned fish (coelacanth *L. chalumnae*) exhibited an N-terminal sequence resembling those found in *C. milii-2* and actinopterygian LEAP2Cs.

3.4. Molecular phylogenetic trees

Molecular phylogenetic analyses of representative vertebrate LEAP2 isoforms (with whole protein regions) showed that LEAP2 sequences were clustered into two main clades according to isoform types in the reconstructed maximum likely (ML) tree (Fig. 3). Within each main clade, branching topologies are generally in agreement with known taxonomic appraisals. The largest clade composed of Actinopterygii (ray-finned fishes) LEAP2As and LEAP2Bs was subdivided into various monophyletic subclades. In this actinopterygian lineage, *A. baerii* formed a monophyletic clade with two other *Acipenser* species, and this chondrostean clade occupied the most primitive position (thereby designated LEAP2AB in this study), followed by a monotypic holostean fish, *L. oculatus* (Lepisosteiformes; Holostei). Within the teleostean clade, LEAP2As and LEAP2Bs formed monophyletic clades, respectively, although they did not receive high bootstrap supports. Teleostean LEAP2A isoforms were recovered according to taxonomic groups at the order or superorder levels, in which acanthopterygians were separated as a monophyletic group from relatively earlier teleost groups such as Protacanthopterygii and Otomorpha. In contrast, the teleostean LEAP2B clade was further subdivided into two distinct subclades according to taxonomic lineages: one was the protacanthopterygian LEAP2Bs, and the other was ostariophysian LEAP2Bs.

The other main clade of the ML tree was subdivided into two subgroups: one was tetrapodian LEAP2 group with one LEAP2-like isoform (*C. milii-1*) from a chondrichthyan species *C. milii* (holocephalian elephant shark), and the other was the fish group comprised of actinopterygian LEAP2Cs, the *C. milii-2* isoform, and a LEAP2-like sequence from *L. chalumnae* (Coelacanthiformes; Sarcopterygii). The monophyletic tetrapodian clade was phylogenetically affiliated with *C. milii-1*, although their relationship was not supported by a high bootstrap score. In the tetrapodian LEAP2 linage, amphibians (Batrachia) was separated from the amniotes. On the other hand, in the fish clade, the two LEAP2-like sequences, respectively from primitive chondrichthyan and sarcopterygian species emerged at the most basal position, followed by the actinopterygian LEAP2C clade. Within the actinopterygian group, chondrosteans (sturgeons; Acipenseriformes) occupied the basal position. Various monophyletic subclades were resolved within a teleostean LEAP2C clade according to taxonomic classifications, while a monotypic *S. formosus* was placed at the outermost position of the teleostean group.

Reconstruction of the phylogenetic tree with a neighbor-joining (NJ) algorithm also resulted in a dichotomic branching pattern according to LEAP2 isoform types. The topology of the NJ tree was similar overall to that of the ML tree above (Suppl. Fig. S3). Different patterns observed in the NJ tree compared with the ML tree are as follows. First,

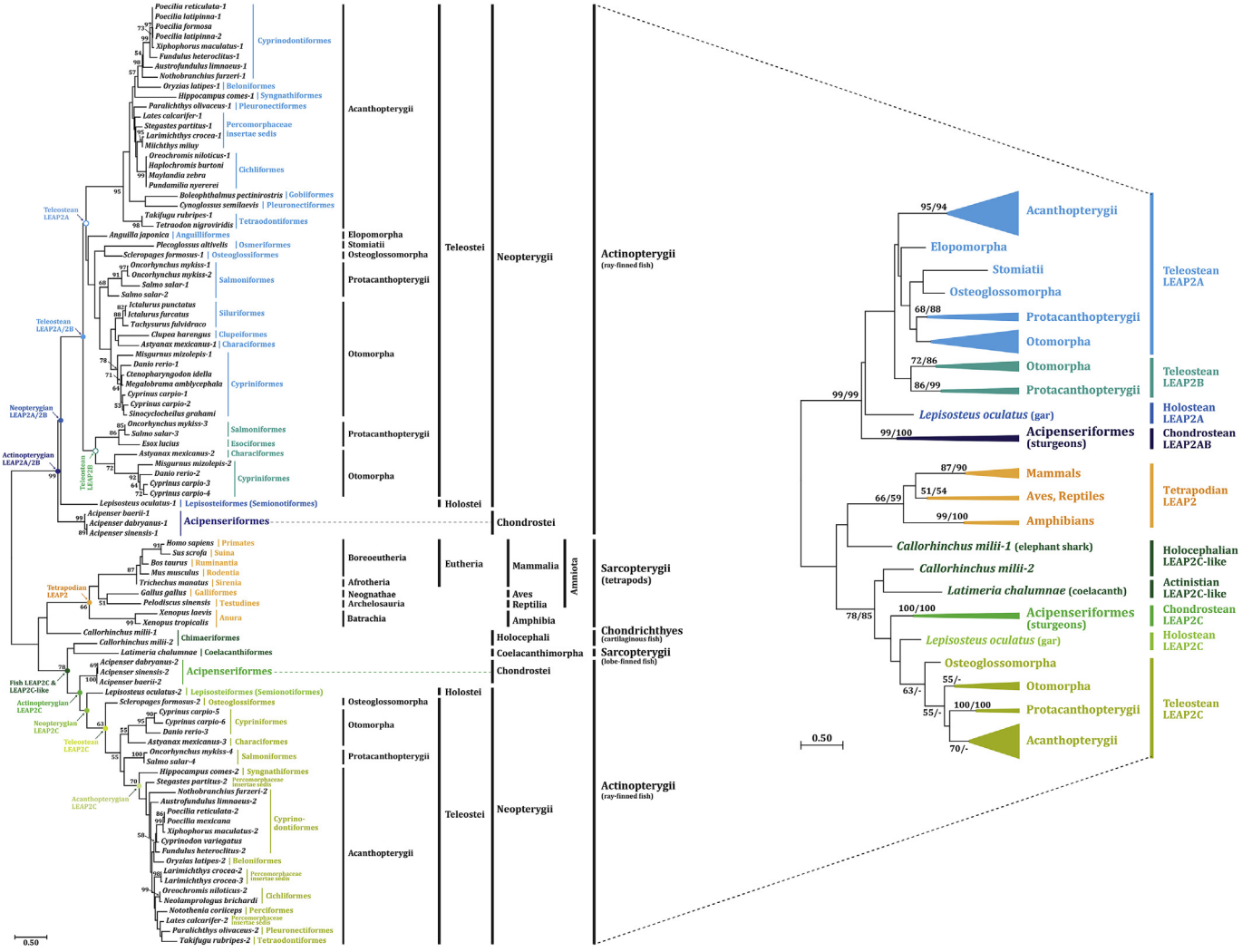

Fig. 3. A molecular phylogenetic tree built using the maximum likely (ML) method to show the phylogenetic relationship of chondrostean LEAP2 isoforms with their orthologs in the vertebrate lineage. The tree was drawn using MEGA software and only bootstrap scores higher than 50% are shown. A compressed tree is also shown at the right for a simplified view. In the compressed tree, bootstrap values from the NJ tree (Suppl. Fig. S3) are also included (ML/NJ).

the *Acipenser* LEAP2s with a holostean (*L. oculatus*) ortholog were placed together at the most basal positions of the actinopterygian clades (LEAP2A/2B and LEAP2C clades). Second, actinopterygian LEAP2Bs were not recovered as a monophyletic group. Third, the *C. mili-1* isoform was not phylogenetically affiliated with a tetrapodian clade; rather, it was placed at the outermost position of the group containing actinopterygian LEAP2Cs. Fourth, tetrapodian LEAP2s were clustered into a monophyletic group, but amniotes were not recovered as a monophyletic group.

3.5. Tissue expression pattern

Based on RT-qPCR, mRNA expression of *A. baerii* LEAP2AB was highly predominant in the liver, while expressed levels in non-liver tissues were quite low or negligible. Besides the liver, muscle exhibits the second highest level of LEAP2AB expression; however, the muscular expression level of *A. baerii* LEAP2AB was less than 3% of the hepatic expression level. Furthermore, *A. baerii* LEAP2C represented a different pattern of tissue expression, in which the intestine showed the highest level of tissue expression, followed by the hepatic expression. Considering the relative mRNA expression levels in the liver between LEAP2AB and LEAP2C, mRNA expression of LEAP2C was more than 4-fold higher than that of LEAP2AB (Fig. 4).

3.6. Expression in developing embryos and early larvae

During embryonic development, *A. baerii* LEAP2AB transcripts were not detectable during early developmental stages until the onset of neurulation. The onset of a small amount of expression was observed at 37 h post insemination (HPI), which corresponded to the elongation of excretory rudiments (EER) stage. Afterward, a significantly increased expression was observed at the heart rudiment formation stage (HR; 59 HPI), which slightly reduced until the prehatching stage (SH – TRH). However, when embryos reached the hatching stage (FH; 119 HPI), the expression was significantly upregulated again, and further increased at 1 day after hatching (DAH) (more than 3-fold relative to that at the hatching stage). The elevated level remained stable until 3 DAH. Subsequently, the expression gradually decreased with prolarval age until 9 DAH. After transition to exogenous feeding at 9 DAH, the expression was partly recovered.

A. baerii LEAP2C transcripts were also significantly elevated at the HR stage but were immediately followed by a decline during intervals from SH to TRH stages. However, upon hatching, the expression of LEAP2C rebounded similarly to the pattern observed with LEAP2AB. During the prolarval stage, *A. baerii* LEAP2C exhibited a modulation pattern different from that of LEAP2AB. Unlike the gradual decrease of LEAP2AB transcripts during the prelarval period, the mRNA expression level of LEAP2AB was continuously increased with prelarval ages up to

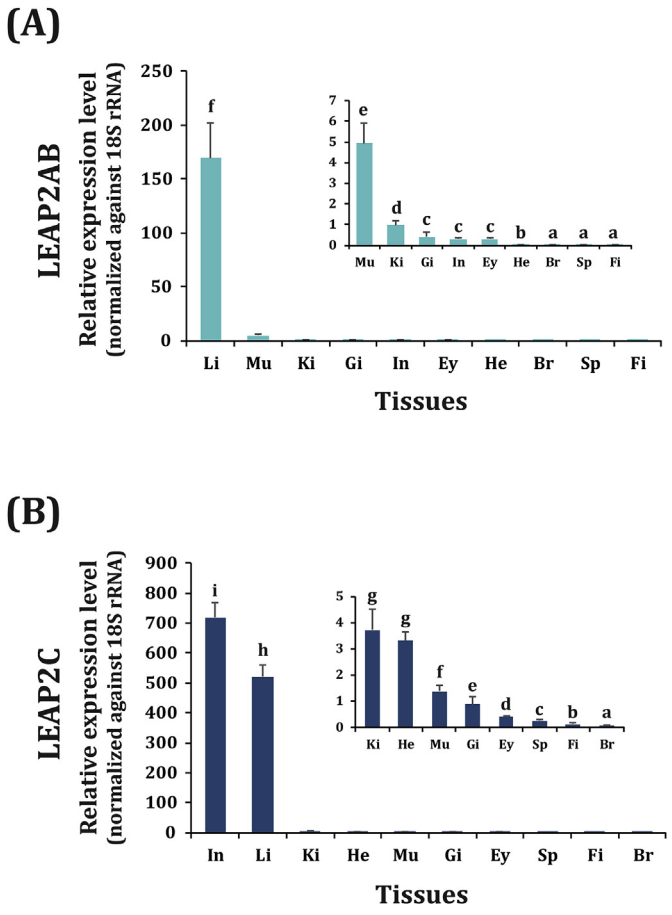

Fig. 4. Tissue distribution patterns and basal expression levels of *Acipenser baerii* LEAP2AB **(A)** and LEAP2C **(B)** transcripts, determined by RT-qPCR assay. Expression levels were normalized against the 18S rRNA gene. Tissue abbreviations are brain (Br), eye (Ey), fin (Fi), gill (Gi), heart (He), intestine (In), kidney (Ki), liver (Li), muscles (Mu), and spleen (Sp). For better visibility, tissues with low expression levels are graphed again with a finer *Y*-axis scale. Statistically different means (± s.d.) within a given isoform are indicated by different letters [$a - f$ in **(A)** and $a - i$ in **(B)**] based on ANOVA followed by Duncan's multiple ranged tests ($P < 0.05$).

7 DAH. Similar to LEAP2AB, the LEAP2C expression was significantly downregulated at 9 DAH and slightly rebounded after the transition to exogenous feeding. The quantitative comparison between LEAP2AB and LEAP2C transcripts during *A. baerii* development indicated that expression levels of LEAP2C were higher than those of LEAP2AB at all examined developmental stages, except the 8-cell and EER stages. The dominant expression of LEAP2C over LEAP2AB transcripts became more pronounced during the prelarval stage (Fig. 5; Suppl. Fig. S4).

3.7. Differential expression in response to stimulatory immune challenges and antimicrobial activity of synthetic peptides

LPS challenge moderately induced both LEPA2AB and LEAP2C transcripts in the kidney but not in the liver or spleen. The maximum induction of LEAP2AB and LEAP2C in the kidney were similar (4.5- and 4.7-fold, respectively) ($P > 0.05$). At 24 HPI, the highest dose and the lowest dose of LPS resulted in significant down-regulation of LEAP2A in the spleen and LEAP2C in the liver, respectively ($P < 0.05$). From the analysis of time course expression pattern in the kidney, both isoforms represented a similar pattern, which was characterized by the upregulation at 12 HPI, further elevation at 18 HPI and then downregulation at subsequent detection points. However, fold-changes of LEAP2AB transcripts relative to PBS control were greater than those of LEAP2C in most detection points ($P < 0.05$) (Fig. 6A). Injection of poly(I:C) induced a slight but statistically significant increase in LEPA2AB transcripts in the liver (maximum 3-fold relative to PBS-injected control) ($P < 0.05$) at 24 HPI. In the kidney, only a lower dose of poly(I:C) (20 μg/g BW) resulted in the upregulation of LEAP2AB transcripts. However, significant upregulation (up to 23-fold) of LEAP2AB expression was observed in the spleen of fish injected with 100 μg/g BW ($P < 0.05$) at 24 HPI. Expression of LEAP2C was not modulated in response to poly(I:C) ($P > 0.05$) irrespective of tissue types. Examination of the time course expression in the spleen up to 48 HPI showed that LEAP2AB was significantly upregulated with the highest induction at 18 HPI and 24 HPI ($P < 0.05$), whereas, in contrast to LEAP2AB, the splenic expression level of LEAP2C was not altered throughout the examination period ($P > 0.05$) (Fig. 6B).

During *A. hydrophila* challenge, no dead individuals were observed until all the sampling had been completed. In the liver, expression of LEAP2AB and LEAP2C were modulated inversely. Expression of LEAP2AB was significantly upregulated during the challenge in which expression levels relative to PBS-injected control were 2-fold at 6 HPI and further increased subsequently (5-fold at 12 HPI and 12-fold at 18 HPI) ($P < 0.05$). Conversely, LEAP2C expression was significantly downregulated during bacterial challenge in the liver ($P < 0.05$). Only 48 h after the challenge, hepatic expression levels of LEAP2C was recovered to the control level. In the kidney, LEAP2AB expression was gradually elevated from 6 to 18 HPI and returned to control levels at 24 HPI ($P < 0.05$), while the highest induction of LEAP2C expression was achieved at 6 HPI followed by a rapid drop to the control level at 18 HPI. Splenic expression of LEAP2AB was quickly upregulated (up to 40-fold at maximum at 6 HPI) upon bacterial injection, followed by a gradual decrease with time until 48 HPI ($P < 0.05$). LEAP2C transcripts were also induced at 6 HPI, but the induced amount (4.5-fold) was much less than LEAP2AB, and moreover, the expression levels of LEAP2C were soon returned to control levels at 12 HPI (Fig. 7A).

Synthetic LEAP2AB peptide displayed antimicrobial activities, which increased as peptide concentration increased, against *B. subtilis*, *S. aureus*, *E. coli*, and *V. anguillarum*. However, two bacterial species *S. iniae* and *A. hydrophila* were not affected by the LEAP2AB in the amounts used in the assay. Meanwhile, the antimicrobial activity of synthetic LEAP2C was observed only against *B. subtilis* and *E. coli*, but not against others. Even it had, its activities against *B. subtilis* and *E. coli* were apparently weaker than those seen in LEAP2AB (Fig. 7B).

4. Discussion

4.1. Peptide sequences and gene structure

Multiple sequence alignments of the mature peptide region indicate that both *A. baerii* isoforms essentially conserved the structural features of vertebrate LEAP2 peptides. Like other LEAP2s, both *A. baerii* LEAP2 isoforms possess four conserved Cys residues in the central core likely to form two disulfide bonds, which are known to be important in the integrity and stability of the core structure through the bracing of a β-hairpin and helix [32]. The *A. baerii* LEAP2s showed multiple hydrophobic residues in their N-terminal regions, similar to other orthologs, which is known to be important for the membrane binding affinity of the LEAP2 peptide [32,33].

Chondrostean sturgeon LEAP2ABs represent higher sequence identity with orthologs from basal neopterygian/teleostean groups [*e.g.*, Holostei (361 mya; based on molecular clock estimation), Osteoglossomorpha (232 mya), and Ostariophysi (210 mya)] compared with those from a relatively recent teleostean group [Acanthomorpha (147 mya)] [34], suggesting that evolutionary diversification of LEAP2A/2Bs has been in broad accordance with speciation history in the actinopterygian group. Meanwhile, intermediate characteristics of chondrostean LEAP2C between teleostean LEAP2Cs and tetrapodian LEAP2s suggest that the chondrostean LEAP2C might reflect the

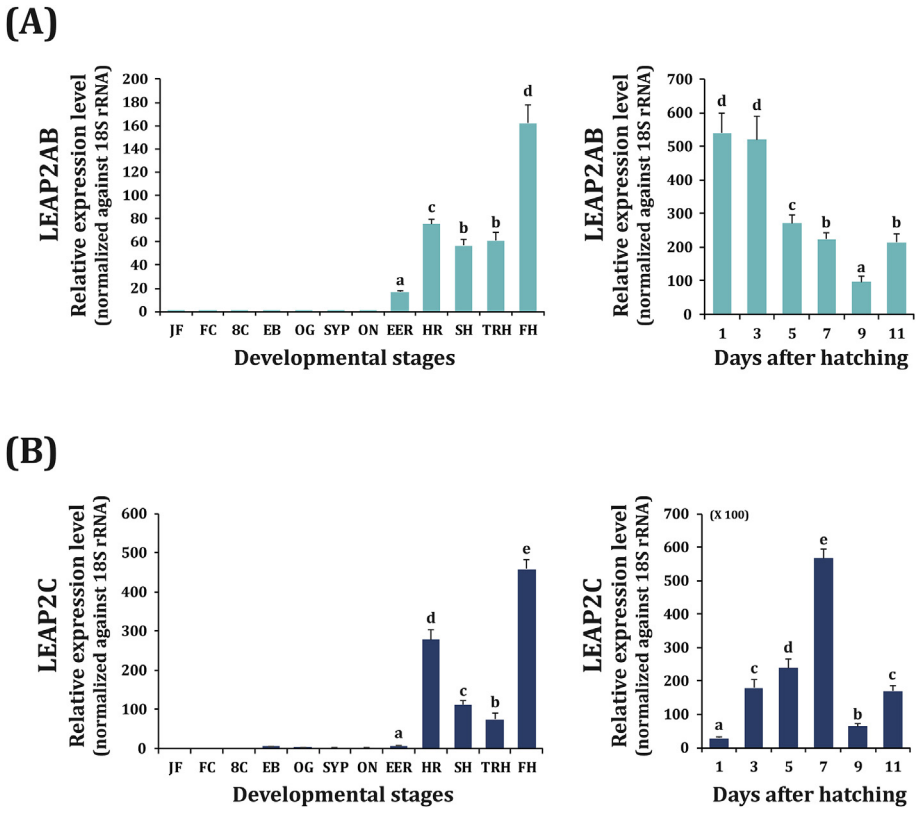

Fig. 5. mRNA expression levels of *Acipenser baerii* LEAP2AB **(A)** and LEAP2C **(B)** isoforms at selected developmental stages and prelarval ages assessed with RT-qPCR assay. Abbreviations for embryonic developmental stages are just fertilized (JF; 0 h post-insemination; HPI), first cleavage (FC; 2 HPI), eight cells (8C; 3.5 HPI), early blastula (EB; 9.6 HPI), onset of gastrulation (OG; 20 HPI), small yolk plug formation (SYP; 28 HPI), onset of neurulation (ON; 33 HPI), elongation of excretory rudiment (EER; 37 HPI), heart rudiment and tail budding (HR; 59 HPI), S-heart formation (SH; 73 HPI), tail end reaching head (TRH; 101 HPI) and first hatching (FH; 119 HPI). Expression levels were normalized against the 18S rRNA gene. Within embryonic development or the prelarval period, statistically different means (± s.d.; as T-bars) are indicated by different letters [*a* – *d* in **(A)** and *a* –*e* in **(B)**] based on ANOVA followed by Duncan's multiple ranged tests ($P < 0.05$). Comparisons of relative expression levels between LEAP2AB and LEAP2C isoforms at a given developmental stage or prelarval age are provided in Suppl. Fig. S4.

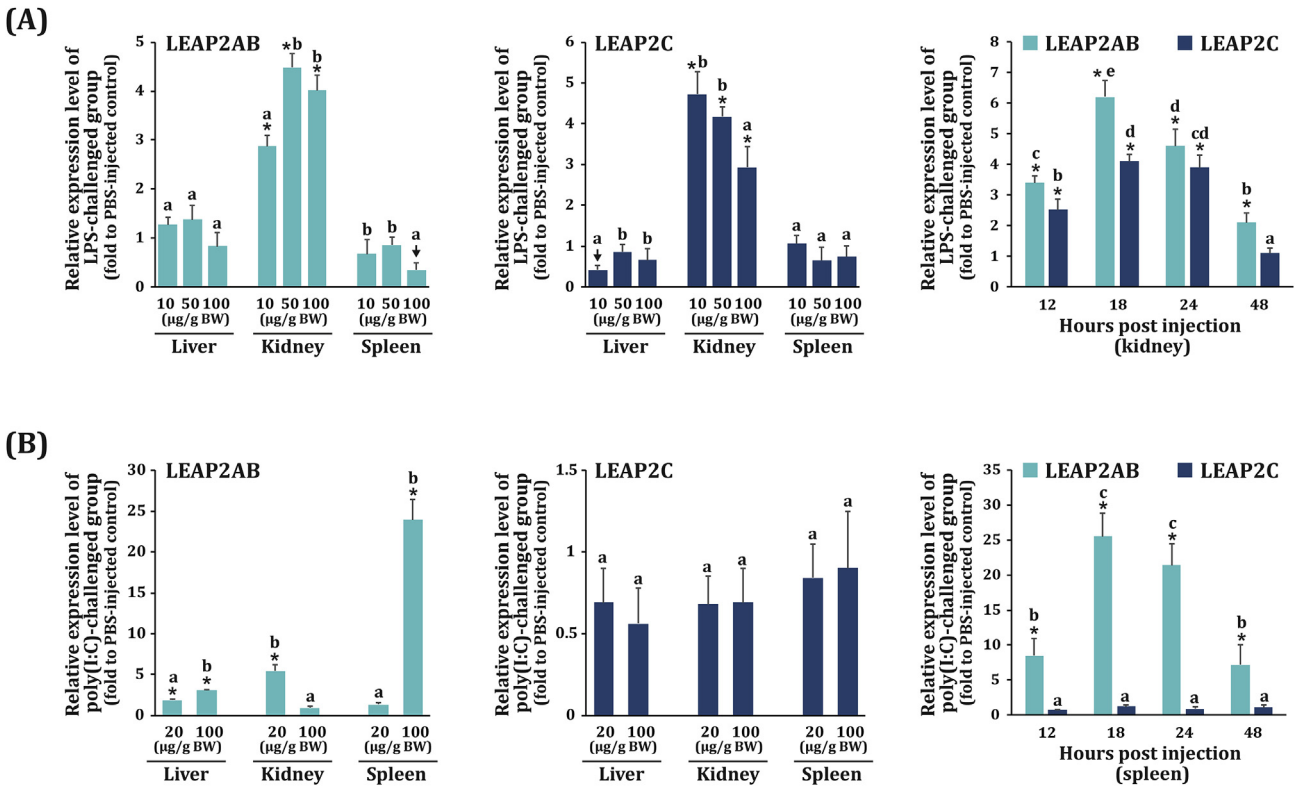

Fig. 6. Differential expression of *Acipenser baerii* LEAP2 isoforms during LPS **(A)** and poly(I:C) **(B)** challenges. Expression levels of challenged groups are presented as fold-changes relative to that of the PBS-injected control group, based on the normalization against 18S rRNA. Significantly induced expression from the basal level of the PBS-injected control group is indicated by an asterisk, while significant downregulation from the control level is indicated by a down arrow above the histogram based on Student's *t*-test at $P < 0.05$. Among challenged groups showing significantly induced LEAP2 expression, statistically different means within a given tissue type are indicated by different letters (*a* – *e*) based on Student's *t*-test and/or ANOVA followed by Duncan's multiple ranged tests ($P < 0.05$).

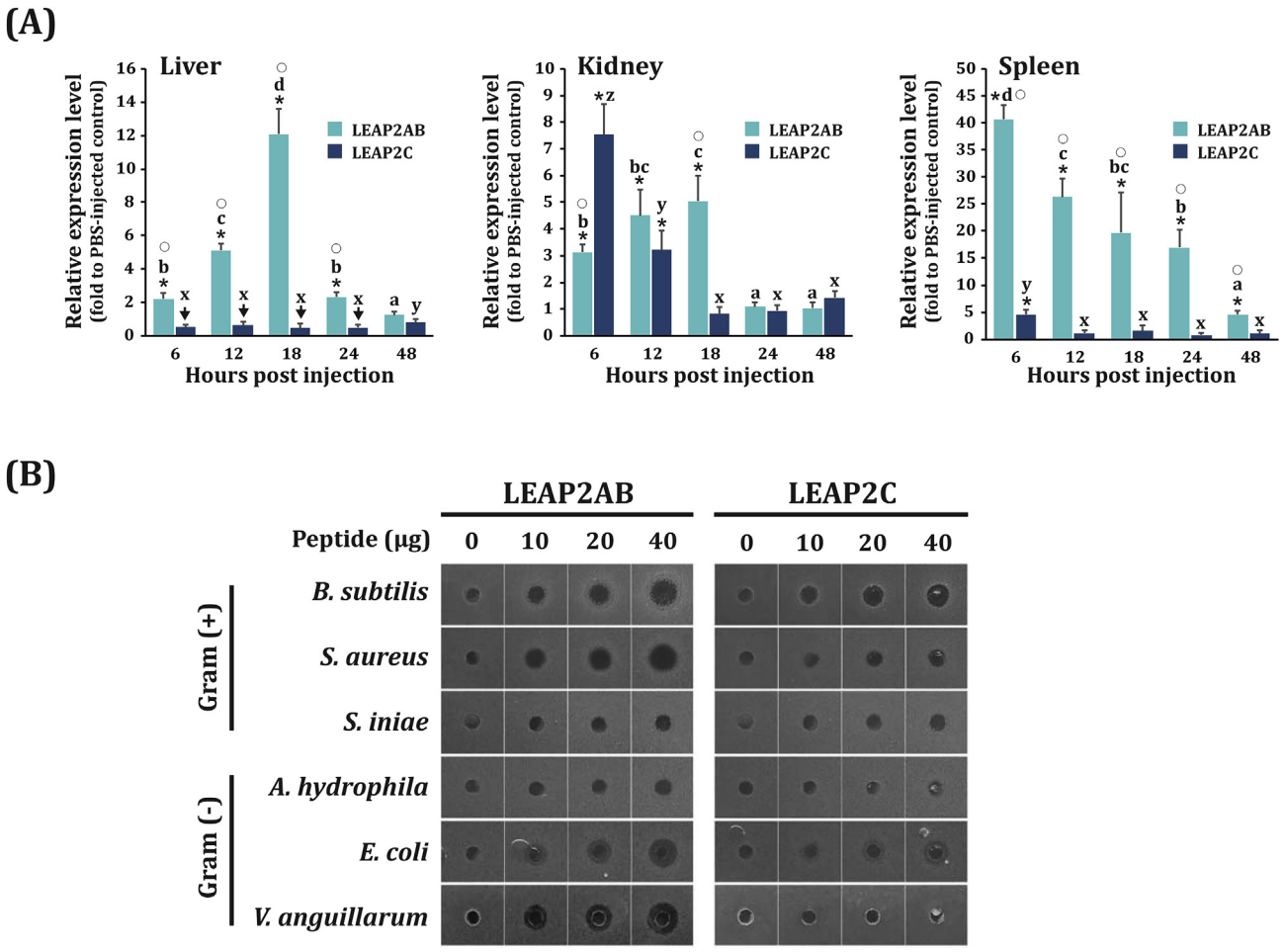

Fig. 7. Transcriptional responses to bacterial challenge **(A)** and antimicrobial activities **(B)** of *Acipenser baerii* LEAP2 isoforms. In **(A)**, expression levels of the *Aeromonas hydrophila*-challenged group are presented as fold-changes relative to PBS-injected controls based on RT-qPCR assay. In each tissue, statistically different means (± s.d.) within a given LEAP2 isoform are indicated by different letters (a – d for LEAP2AB and x – z for LEAP2C) based on ANOVA followed by Duncan's multiple ranged tests ($P < 0.05$). Asterisks and down arrows indicate statistically elevated and depressed expression levels of *A. hydrophila*-injected groups, respectively, as compared with the expression level of the PBS-injected control based on Student's t-test ($P < 0.05$). Statistical difference in fold-change between LEAP2AB and LEAP2C at each detection point is indicated by open circle on the histogram for the LEAP2AB isoform based on Student's t-test ($P < 0.05$). In **(B)**, each peptide was tested for the activity at a quantity ranging from 0 to 40 μg using ultrasensitive radial diffusion assay. Bacteria used in this study were gram-positive bacteria, *Bacillus subtilis* KCTC 1021, *Staphylococcus aureus* KCTC 1621, *Streptococcus iniae* FD 5228, and gram-negative bacteria, *A. hydrophila* KCTC 2358, *Escherichia coli* ML 35, and *Vibrio anguillarum* KCTC 2711.

primitive shape of LEAP2C, which is similar to previous findings with other genes from primitive fishes [3,35,36].

The tripartite organization of both *A. baerii* LEAP2 isoform genes is a common architecture found in all vertebrate orthologs, and furthermore, the exon/intron lengths in each *A. baerii* LEAP2 isoform is also highly similar to those reported in other sturgeon species [27]. Moreover, even though not described by the previous study, all the three *Acipenser* LEAP2AB isoforms, including the *A. baerii* LEAP2AB of this study identically possess a noncanonical G**C**-AG exon-intron boundary sequence (*i.e.,* GC-AG intron) in the intron-2, which is not common to previously known vertebrate LEAP2s. Although the potential involvement of this noncanonical sequence in the regulation of *Acipenser* LEAP2 is unclear, the GC donor splice signals have been proposed to have important roles in the regulation of alternative splicing of mammalian genes [37], suggesting the need for testing the potential production of alternatively spliced forms of sturgeon LEAP2ABs in the future.

4.2. Evolution and phylogeny

The branching patterns of phylogenetic trees for actinopterygian LEAP2s in this study are fairly congruent with those previously suggested for phylogenetic classification and speciation of bony fishes using other nuclear genes, mtDNA, or transcriptomic sequences [34,38,39], suggesting that LEAP2 could be a useful candidate phylogenetic marker to trace the evolutionary history of actinopterygians. From previous and present studies, almost all bony fishes are thought to possess two isoforms LEAP2A and LEAP2C, while LEAP2B isoforms have been limited to only a few ostariophysian and protacanthopterygian species. However, the origin of LEAP2B is currently difficult to hypothesize because the monophyletic recovery of LEAP2Bs is inconsistent and depends on phylogenetic reconstruction methods. If the protacanthopterygian and ostariophysian LEAP2Bs share a common ancestor (as in the present ML tree), the emergence of the ancestral LEAP2B should be no later than the Otocephala-Euteleostei divergence from the Clupeocephala (230–240 mya). Alternatively, if the two subgroups of LEAP2Bs are truly polyphyletic (as in the present NJ tree), their emergence might be dated back to about 80–100 mya, considering the molecular clock age estimation of these orders [Salmoniformes (88 mya), Esociformes (102 mya), Cypriniformes (95 mya), and Characiformes (99 mya)] [34,40]. Furthermore, species such as salmonids and carp, which are known to have undergone additional genome

duplication events (50–80 mya at the base of Salmoniformes and 5.6–11.3 mya in a closely related ancestor of the carp [41], representing duplicated copies within a given isoform (*e.g.,* each two copies of LEAP2A in salmonids, and each two copies of LEAP2A, 2B and 2C in carp).

In the ML tree, chondrostean LEAP2AB isoforms occupied the most basal branch in the actinopterygian lineage, suggesting that they would be prototypes of actinopterygian LEAP2A/2B isoforms, which is in agreement with phylogenetic positions of chondrostean sturgeons branched-off from the class Actinopteri (*i.e.,* the separation from the subclass Neopterygii; 360 mya). Our proposed phylogenetic hypothesis is somewhat dissimilar to a previous report suggesting that *A. dabryanus* and *A. sinensis* LEAP2 isoforms should be LEAP2B based on their affiliation with salmoniform LEAP2Bs [27].

Meanwhile, fish LEAP2C (and 2C-like) isoforms represented a closer phylogenetic affiliation to tetrapodian LEAP2s rather than being clustered with the fish LEAP2A/2B group, suggesting that the two fish LEAP2 isoforms (LEAP2A/2B and LEAP2C) might have different evolutionary backgrounds. In the ML tree, the most primitive position in the actinopterygian LEAP2C group was occupied by chondrostean LEAP2C, followed by a holostean ortholog and then teleostean LEAP2Cs, while the most basal clade contained a holostean ortholog in addition to chondrostean LEAP2Cs in the NJ tree. However, the present phylogenetic analysis including other primitive LEAP2-like isoforms (two isoforms from Holocephali and one isoform from Coelacanthiformes) suggest that the LEAP2 is a truly ancient molecule whose evolutionary origin might date back to at least the late Silurian period (about 420 mya) when early Eugnathostomata diverged into two groups, Chondrichthyes and Osteichthyes [42–44]. In the ML tree, but less clearly in NJ tree than in ML tree, phylogenetic separation of the two isoforms from a primitive holocephalian species (*i.e., C. milii-1* and *C. milii-2*) may imply that they have been derived from an ancestral divergence event and undergone different evolutionary paths in the vertebrate lineage (*e.g., C. milii-1* affiliated with the tetrapodian LEAP2 lineage, and *C. milii-2* with a fish LEAP2C lineage). A previous genome study reported that this holocephalian species (*C. milii*) genome might be the slowest evolving of all known vertebrates with extensive synteny conservation with tetrapod genomes [42]. The osteichthyan group appeared in the late Silurian period and did not take long split into two clades [i.e., the lobe-finned (Sarcopterygii) and the ray-finned (Actinopterygii) fishes]. This split is posited to have occurred no later than 419 mya (during the early Devonian period) [45]. Although the relationship was not supported by high bootstrap values in both the ML and NJ trees of this study, the phylogenetic affiliation of sarcopterygian (coelacanth *L. chalumnae*) LEAP2 with *C. milii-2* (but not with *C. milii-1*), and together with actinopterygian LEAP2Cs suggests that the ancestral LEAP2C form might have appeared before the actinopterygian-sarcopterygian split [45–47]. However, further mining of other isoforms from the sarcopterygian species showing the genetic affiliation to either tetrapodian LEAP2 or actinopterygian LEAP2A/2B is needed to solidify this hypothesis.

4.3. Potential subfunctionalization in tissue and developmental expression

Based on the RT-qPCR assay, the notably robust expression of LEAP2C in the intestine (higher than in the liver) which was different from the LEAP2AB isoform having only a minute expression level in all the non-liver tissues, suggesting differentiated or divergent roles of the two isoforms in *A. baerii* tissues under non-stimulated conditions. A relatively much higher level of LEAP2C than LEAP2AB in the liver (more than 4-fold), as well as in the intestine (more than 500-fold), may also be indicative, at least in part, that LEAP2C plays a major role under non-stimulated conditions. Tissue distribution patterns of LEAP2 isoforms have also been reported to be largely species-specific in teleosts. Although the expression patterns of teleostean LEAP2C were limited to only a few species, tissue expressions among teleosts are highly diversified in a species-specific manner, and consequently, it is difficult to generalize patterns in a lineage- or isoform-dependent fashion [22,23,26,48]. Also, within the genus *Acipenser*, the expression pattern found in *A. baerii* is not highly accordant with that previously reported in *A. dabryanus* [27]. The most striking difference was that one isoform (termed LEAP2B in the previous study) from *A. dabryanus* was not clearly detectable in various tissues, including the liver. In addition, the expression of *A. dabryanus* LEAP2C in the intestine was only moderate (40-fold lower in the intestine than in the liver) [27]. Collectively, the tissue expression patterns of LEAP2 isoforms in Actinopterygii, including the chondrostean group might have been diversified mostly at the species level.

Both *A. baerii* LEAP2 isoforms were dynamically regulated during embryonic development and the prolarval period (from hatch to yolk sac absorption). During embryonic development, both isoforms displayed a similar onset of expression (EER to HR stages), which is also broadly similar to previous findings with ostariophysian LEAP2As (Siluriformes and Cypriniformes) in that the robust expression of LEAP2s would occur mainly in later developmental stages rather than during early development from cleavages to gastrulation [22,24]. However, some cypriniform species showed considerable expression of LEAP2 transcripts as early as the 16-cell stage (in *Ctenopharyngodon idella* [21]) or the mid-gastrula stage (in *Megalobrama amblycephala*; [49]). When *A. baerii* embryos reached the HR stage, both isoforms represented the first peak of expression. This stage corresponds to the interval when the rudimentary heart progressively develops to form the S-shaped heart. The formation of the S-shaped heart is a critical sign for initiating heartbeat to allow the active circulation of biomolecules through blood vessel networks [28,50,51]. Hence, the robust expression of LEAP2 mRNAs at the HR stage might be regarded as the groundwork to prepare LEAP2s for the onset of circulation from the SH stage. Afterward, both *A. baerii* LEAP2 isoforms showed the second peak of expression at hatching. The significant elevation of LEAP2 expression around the hatching stage has also been reported in other teleost species (ostariophysian LEAP2As), and this phenomenon could be generally explained by the preparation of the protective function for hatched larvae that are no longer sheltered by the egg membrane [21,22,49]. After hatching, the expression patterns of the two LEAP2 isoforms were significantly different from one another during the prelarval period, in which LEAP2AB showed a gradual decrease of expression, whereas the LEAP2C exhibited a sharp increase. In a quantitative viewpoint, the LEAP2C was always a dominant isoform over LEAP2AB, suggesting that LEAP2C, rather than LEAP2AB, is the main isoform involved with prolarval physiology. However, at 9 DPH, significant downregulation of LEAP2 expression was observed for both LEAP2 isoforms. This age corresponds to the end-phase of the prolarval stage: prolarvae absorbed yolk materials and were ready to evacuate the yolk plug (also called the pigment plug) [29,50]. During this period, *A. baerii* prolarvae display a typical behavioral appearance, characterized by conspicuous inactivity, remaining motionless and scattered across the bottom of the tank (called post-schooling behavior) [52]. Prolarvae at this stage are proposed to divert almost all their energy into the final preparation of the digestive system in order to enter the larval stage (*i.e.,* transition from the endogenous nutrition system to exogenous feeding) [52,53].

4.4. Isoform-dependent responses to immune challenges and antimicrobial activities

Transcriptional responses of LEAP2 isoforms during stimulatory challenges were isoform-specific and tissue-dependent, in which, except for a moderate increase in both LEAP2AB and LEAP2C transcripts in the kidney during LPS and *A. hydrophila* challenges, the overall response patterns of the isoforms were dissimilar to each other. As demonstrated with poly(I:C) challenge, only LEAP2AB, but not LEAP2C, was significantly upregulated, suggesting LEAP2AB may be a main isoform

associated with the cellular pathways involved in the protective function against viral invasion. From the bacterial challenge with *A. hydrophila*, both *A. baerii* LEAP2 isoforms exhibited an early acute phase response, which is similarly observable in teleost fishes [18,20,21,48]. However, their modulatory patterns were different from one another. In the liver, the modulation diverged for the two isoforms, where LEAP2AB was upregulated while LEAP2C was downregulated. In the kidney, mRNA expression of both isoforms increased as in the LPS challenge; however, the temporal patterns during the early phase (up to 18 HPI) were oppositely modulated. Finally, in the spleen, the amount of induction during the bacterial challenge was mostly observable only for LEAP2AB, rather than LEAP2C. Collectively, findings from the immune challenges suggest that two *A. baerii* LEAP2 isoforms have undergone significant subfunctionalization with regard to their roles in the innate immune system, and also indicate that the LEAP2AB isoform, rather than LEAP2C would be more closely involved in the acute response to microbial invasion in this sturgeon species. However, a previous study has claimed that *A. dabryanus* LEAP2C would be the immune-responsive antimicrobial peptide contributing to the defense against pathogenic bacterial invasion based on its transcriptional upregulation during *A. hydrophila* challenge [27]. However, a lack of parallel comparison to its paralog counterpart isoform (LEAP2B) in *A. dabryanus* makes it difficult to fully evaluate the isoform-dependent relevance to innate immunity between the two chondrostean sturgeon species [27]. Potential subfunctionalization between LEAP2 isoforms have also been reported in teleosts based on isoform-specific modulations in response to immune challenges in different tissues [22,26,48].

From the antimicrobial activity test using synthetic mature peptides, LEAP2AB was proven to be more potent than LEAP2C, considering the kinds of bacterial species affected and the strength of antimicrobial activity. Of six bacterial species tested, LEAP2AB have shown antimicrobial activities against four bacterial species (*B. subtilis, S. aureus, E. coli*, and *V. anguillarum*) in a peptide concentration-dependent fashion. However, antimicrobial activity of LEAP2C was observable against only two bacterial species (*B. subtilis* and *E. coli*) that were affected by LEAP2AB also. Moreover, antimicrobial activities of LEAP2C against those two bacterial species were much weaker than those of LEAP2AB. Collectively, finding with antimicrobial activity assay also supports our hypothesis on their sub-functionalized roles in innate immunity-related physiology. Although functional antimicrobial activities of all the actinopterygian LEAP2s have not been verified in an isoform-dependent manner, our finding is broadly congruent with that the LEAP2 isoform that has been reported to exhibit actual antimicrobial activity in actinopterygian species should be mostly classified to LEAP2A/2B isoforms rather than LEAP2C in our molecular phylogenetic analysis [18,20,21,25,54]. The single exception to report antimicrobial activity of LEAP2C is from the yellow croaker *Larimichthys polyactis* [48]. Antimicrobial activity of the LEAP2 peptide has been reported to be closely associated with the membrane binding affinity that is governed by the hydrophobic residues in its N-terminal region, whereas the C-terminal region and cysteine disulfide bonds in the core region are irrelevant and/or non-essential for antimicrobial activity of the LEAP2 peptide [32,33]. Within the structure-functional context, the antimicrobial activity of actinopterygian LEAP2A/2Bs could broadly agree because they represent a greater resemblance to human LEAP2 in the hydrophobic N-terminal region, although the whole proteins of LEAP2Cs show a closer phylogenetic affiliation to human LEAP2 than do LEAP2A/2Bs.

Meanwhile, in the comparison between mRNA expression and antimicrobial activity assay, synthetic LEAP2AB peptides do not represent antimicrobial activity against *A. hydrophila* in spite of transcriptional upregulation of LEAP2AB gene during the challenge with the same bacterial strain. The clear reason responsible for this unexpected finding has remained to be further studied, although this is likely related to the *in vitro* nature of the antibacterial activity assay. Another possible, but untested, explanation is that the stimulated expression of LEAP2 during *A. hydrophila* challenge could be associated with its roles in the modulation of other immune factors and local anti-inflammatory function [18–20,55,56], rather than the direct bactericidal action against *A. hydrophila*. A recent our study with sturgeon hepcidin (LEAP1) has proposed that increased hepcidin expression during bacterial infection in tissues representing very low basal expression levels might be more closely related with local protective function(s) with the regulation of iron flux than with humoral bacteria-killing action, since the seemingly great fold changes of expression in those tissues would reflect only minute increases of absolute amounts of AMPs [15].

Recently, the primary physiological role of mammalian LEAP2 has been proven to be the antagonistic regulation of energy metabolism through its interconnection with ghrelin, a key endocrine hormone [57,58]. Based on the new information from mammalian LEAP2, it is, therefore, of value to examine the possibility that actinopterygian LEAP2 isoforms (*i.e.,* one or both isoforms) may share functional orthology with mammalian LEAP2 regarding the involvement in glucose metabolism as a hormonal regulator, which could be an important clue to better hypothesize the evolutionary history of LEAP2 in vertebrates.

5. Conclusion

Two functionally expressed LEAP2 isoforms were characterized in a chondrostean surgeon species, *A. baerii*. *A. baerii* LEAP2 isoforms share common structural features with other vertebrate orthologs at both peptide and genomic levels. *A. baerii* LEAP2 isoforms phylogenetically occupy the most basal position in the actinopterygian lineage and represent some intermediate characters between teleostean and tetrapodian LEAP2s. Based on phylogenetic analysis, including orthologs from extant primitive fish species, the evolutionary origin of ancestral LEAP2 in vertebrate groups should date back to no later than the actinopterygian-sarcopterygian split (or even the Osteichthyes-Chondrichthyes split). Gene expression and antimicrobial activity assays suggested that the two *A. baerii* LEAP2 isoforms have undergone substantial subfunctionalization of their roles in the developmental and the innate immune system. Overall, the LEAP2AB isoform would be more closely related with innate immune response to pathogenic invasion, while LEAP2C might have another physiological role(s) under non-stimulated, basal conditions. Results from this study could be a useful basis not only to gain deeper insight into the evolutionary mechanism of LEAP2 in the actinopterygian lineage but also to better understand the innate immunity of chondrosteans, which are of potential importance in health management of commercially important sturgeon species.

Acknowledgments

This research was supported by a grant from the Korea Institute of Marine Science & Technology (KIMST), funded by the Ministry of Oceans and Fisheries (Project #20170327).

Appendix A. Supplementary data

Supplementary data to this article can be found online at https://doi.org/10.1016/j.fsi.2019.07.040.

References

[1] V.J. Birstein, R. Hanner, R. DeSalle, Phylogeny of the Acipenseriformes: cytogenetic and molecular approaches, Environ. Biol. Fish. 48 (1997) 127–155.
[2] D.S. Kim, Y.K. Nam, J.K. Noh, C.H. Park, F.A. Chapman, Karyotype of North American shortnose sturgeon *Acipenser brevirostrum* with the highest chromosome number in the Acipenseriformes, Ichthyol. Res. 52 (2005) 94–97 http://doi.org/10.1007/s10228-004-0257-z.
[3] Y.S. Cho, S.E. Douglas, J.W. Gallant, K.Y. Kim, D.S. Kim, Y.K. Nam, Isolation and characterization of cDNA sequences of L-gulono-gamma-lactone oxidase, a key enzyme for biosynthesis of ascorbic acid, from extant primitive fish groups, Comp. Biochem. Physiol., B 147 (2007) 178–190 http://doi.org/10.1016/j.cbpb.2007.01.

001.
[4] V.A. Trifonov, S.S. Romanenko, V.R. Beklemisheva, L.S. Biltueva, A.I. Makunin, N.A. Lemskaya, A.I. Kulemzina, R. Stanyon, A.S. Graphodatsky, Evolutionary plasticity of acipenseriform genomes, Chromosoma 125 (2016) 661–668 https://doi.org/10.1007/s00412-016-0609-2.
[5] M.A.H. Webb, S.I. Doroshov, Importance of environmental endocrinology in fisheries management and aquaculture of sturgeons, Gen. Comp. Endocrinol. 170 (2011) 313–321 http://doi.org/10.1016/j.ygcen.2010.11.024.
[6] H. Yu-ping, W. Di, A review of sturgeon virosis, J. For. Res. 16 (2005) 79–82 https://doi.org/10.1007/BF02856862.
[7] I.S. Shchelkunov, T.I. Shchelkunova, A.I. Shchelkunov, Y.P. Kolbassova, L.V. Didenko, A.P. Bykovsky, First detection of a viral agent causing disease in farmed sturgeon in Russia, Dis. Aquat. Org. 86 (2009) 193–203 https://doi.org/10.3354/dao02124.
[8] W. Yang, A. Li, Isolation and characterization of *Streptococcus dysgalactiae* from diseased *Acipenser schrenckii*, Aquaculture 294 (2009) 14–17 https://doi.org/10.1016/j.aquaculture.2009.05.018.
[9] S. Ciulli, E. Volpe, S. Sirri, P.L. Passalacqua, F.C. Bianchi, P. Serratore, L. Mandrioli, Outbreak of mortality in Russian (*Acipenser gueldenstaedtii*) and Siberian (*Acipenser baerii*) sturgeons associated with sturgeon nucleo-cytoplasmatic large DNA virus, Vet. Microbiol. 191 (2016) 27–34 https://doi.org/10.1016/j.vetmic.2016.05.012.
[10] L. Bigarré, M. Lesne, A. Lautraite, V. Chesneau, A. Leroux, M. Jamin, P.M. Boitard, A. Toffan, M. Preao, S. Labrut, P. Daniel, Molecular identification of iridoviruses infecting various sturgeon species in Europe, J. Fish Dis. 40 (2017) 105–118 https://doi.org/10.1111/jfd.12498.
[11] R. Zhu, H.J. Du, S.Y. Li, Y.D. Li, H. Ni, X.J. Yu, Y.Y. Yang, Y.D. Fan, N. Jiang, L.B. Zeng, X.G. Wang, De novo annotation of the immune-enriched transcriptome provides insights into immune system genes of Chinese sturgeon (*Acipenser sinensis*), Fish Shellfish Immunol. 55 (2016) 699–716 https://doi.org/10.1016/j.fsi.2016.06.051.
[12] H. Zhu, R. Song, X. Wang, H. Hu, Z. Zhang, Peritoneal bacterial infection repressed the expression of IL17D in Siberia sturgeon a chondrostean fish in the early immune response, Fish Shellfish Immunol. 64 (2017) 39–48 https://doi.org/10.1016/j.fsi.2017.03.011.
[13] K. Luo, J. Di, P. Han, S. Zhang, L. Xia, G. Tian, W. Zhang, D. Dun, Q. Xu, Q. Wei, Transcriptome analysis of the critically endangered Dabry's sturgeon (*Acipenser dabryanus*) head kidney response to *Aeromonas hydrophila*, Fish Shellfish Immunol. 83 (2018) 249–261 https://doi.org/10.1016/j.fsi.2018.09.044.
[14] Z. Qi, S. Wang, X. Zhu, Y. Yang, P. Han, Q. Zhang, S. Zhang, R. Shao, Q. Xu, Q. Wei, Molecular characterization of three toll-like receptors (TLR21, TLR22, and TLR25) from a primitive ray-finned fish Dabry's sturgeon (*Acipenser dabryanus*), Fish Shellfish Immunol. 82 (2018) 200–211 https://doi.org/10.1016/j.fsi.2018.08.033.
[15] C.H. Kim, E.J. Kim, Y.K. Nam, Chondrostean sturgeon hepcidin: an evolutionary link between teleost and tetrapod hepcidins, Fish Shellfish Immunol. 88 (2019) 117–125 https://doi.org/10.1016/j.fsi.2019.02.045.
[16] A. Krause, R. Sillard, B. Kleemeier, E. Klüver, E. Maronde, J.R. Conejo-García, W.G. Forssmann, P. Schulz-Knappe, M.C. Nehls, F. Wattler, S. Wattler, K. Adermann, Isolation and biochemical characterization of LEAP-2, a novel blood peptide expressed in the liver, Protein Sci. 12 (2003) 143–152 https://doi.org/10.1110/ps.0213603.
[17] V. Rajanbabu, J.Y. Chen, Applications of antimicrobial peptides from fish and perspectives for the future, Peptides 32 (2011) 415–420 https://doi.org/10.1016/j.peptides.2010.11.005.
[18] H.X. Li, X.J. Lu, C.H. Li, J. Chen, Molecular characterization of the liver-expressed antimicrobial peptide 2 (LEAP-2) in a teleost fish, *Plecoglossus altivelis*: antimicrobial activity and molecular mechanism, Mol. Immunol. 65 (2015) 406–415 https://doi.org/10.1016/j.molimm.2015.02.022.
[19] B.A. Katzenback, Antimicrobial peptides as mediators of innate immunity in teleosts, Biology 4 (2015) 607–639 https://doi.org/10.3390/biology4040607.
[20] J. Chen, Q. Chen, X.J. Lu, J. Chen, The protection effect of LEAP-2 on the mudskipper (*Boleophthalmus pectinirostris*) against *Edwardsiella tarda* infection is associated with its immunomodulatory activity on monocytes/macrophages, Fish Shellfish Immunol. 59 (2016) 66–76 https://doi.org/10.1016/j.fsi.2016.10.028.
[21] F. Liu, J.L. Li, G.H. Yue, J.J. Fu, Z.F. Zhou, Molecular cloning and expression analysis of the liver-expressed antimicrobial peptide 2 (LEAP-2) gene in grass carp, Vet. Immunol. Immunopathol. 133 (2010) 133–143 https://doi.org/10.1016/j.vetimm.2009.07.014.
[22] S.Y. Lee, Y.K. Nam, Gene structure and expression characteristics of liver-expressed antimicrobial peptide-2 isoforms in mud loach (*Misgurnus mizolepis*; Cypriniformes), Fish. Aquat. Sci. 20 (2017) 1–11 https://doi.org/10.1186/s41240-017-0076-6.
[23] Y.A. Zhang, J. Zou, C.I. Chang, C.J. Secombes, Discovery and characterization of two types of liver-expressed antimicrobial peptide 2 (LEAP-2) genes in rainbow trout, Vet. Immunol. Immunopathol. 101 (2004) 259–269 https://doi.org/10.1016/j.vetimm.2004.05.005.
[24] B. Bao, E. Peatman, P. Xu, P. Li, H. Zeng, C. He, Z. Liu, The catfish liver-expressed antimicrobial peptide 2 (LEAP-2) gene is expressed in a wide range of tissues and developmentally regulated, Mol. Immunol. 43 (2006) 367–377 https://doi.org/10.1016/j.molimm.2005.02.014.
[25] T. Liu, Y. Gao, R. Wang, T. Xu, Characterization, evolution and functional analysis of the liver-expressed antimicrobial peptide 2 (LEAP-2) gene in miiuy croaker, Fish Shellfish Immunol. 41 (2014) 191–199 https://doi.org/10.1016/j.fsi.2014.08.010.
[26] G. Yang, H. Guo, H. Li, S. Shan, X. Zhang, J.H.W.M. Rombout, L. An, Molecular characterization of LEAP-2 cDNA in common carp (*Cyprinus carpio* L.) and the differential expression upon a *Vibrio anguillarum* stimulus; indications for a significant immune role in skin, Fish Shellfish Immunol. 37 (2014) 22–29 https://doi.org/10.1016/j.fsi.2014.01.004.
[27] S. Zhang, Q. Xu, H. Du, Z. Qi, Y. Li, J. Huang, J. Di, Q. Wei, Evolution, expression, and characterisation of liver-expressed antimicrobial peptide genes in ancient chondrostean sturgeons, Fish Shellfish Immunol. 79 (2018) 363–369 https://doi.org/10.1016/j.fsi.2018.05.023.
[28] C.H. Park, S.Y. Lee, D.S. Kim, Y.K. Nam, Embryonic development of Siberian sturgeon *Acipenser baerii* under hatchery conditions: an image guide with embryological descriptions, Fish. Aquat. Sci. 16 (2013) 15–23 http://doi.org/10.5657/fas.2013.0015.
[29] C.H. Park, S.Y. Lee, D.S. Kim, Y.K. Nam, Effects of incubation temperature on egg development, hatching and pigment plug evacuation in farmed Siberian sturgeon *Acipenser baerii*, Fish. Aquat. Sci. 16 (2013) 25–34 http://doi.org/10.5657/fas.2013.0025.
[30] K.J. Livak, T.D. Schmittgen, Analysis of relative gene expression data using real-time quantitative PCR and the $2^{-\Delta\Delta CT}$ method, Methods 25 (2001) 402–408 https://doi.org/10.1006/meth.2001.1262.
[31] T.D. Schmittgen, K.J. Livak, Analyzing real-time PCR data by the comparative CT method, Nat. Protoc. 3 (2008) 1101–1108.
[32] S.T. Henriques, C.C. Tan, D.J. Craik, R.J. Clark, Structural and functional analysis of human liver-expressed antimicrobial peptide 2, Chembiochem 11 (2010) 2148–2157 https://doi.org/10.1002/cbic.201000400.
[33] A. Hocquellet, B. Odaert, C. Cabanne, A. Noubhani, W. Dieryck, G. Joucla, C. Le Senechal, M. Milenkov, S. Chaignepain, J. Schmitter, S. Claverol, X. Santarelli, E.J. Dufourc, M. Bonneu, B. Garbay, P. Costaglioli, Structure-activity relationship of human liver-expressed antimicrobial peptide 2, Peptides 31 (2010) 58–66 https://doi.org/10.1016/j.peptides.2009.10.006.
[34] T.J. Near, R.I. Eytan, A. Dornburg, K.L. Kuhn, J.A. Moore, M.P. Davis, P.C. Wainwright, M. Friedman, W.L. Smith, Resolution of ray-finned fish phylogeny and timing of diversification, Proc. Natl. Acad. Sci. U.S.A. 109 (2012) 13698–13703 https://doi.org/10.1073/pnas.1206625109.
[35] N. Suzuki, K. Ueda, H. Sakamoto, Y. Sasayama, Fish calcitonin genes: primitive bony fish genes have been conserved in some lower vertebrates, Gen. Comp. Endocrinol. 113 (1999) 369–373 https://doi.org/10.1006/gcen.1998.7215.
[36] Y.S. Cho, B.N. Choi, E.M. Ha, K.H. Kim, S.K. Kim, D.S. Kim, Y.K. Nam, Shark (*Scyliorhinus torazame*) metallothionein: cDNA cloning, genomic sequence, and expression analysis, Mar. Biotechnol. 7 (2005) 350–362 https://doi.org/10.1007/s10126-004-0043-y.
[37] A. Churbanov, S. Winters-Hilt, E.V. Koonin, I.B. Rogozin, Accumulation of GC donor splice signals in mammals, Biol. Direct 3 (2008) 30 http://doi.org/10.1186/1745-6150-3-30.
[38] R. Betancur-R, E.O. Wiley, G. Arratia, A. Acero, N. Baily, M. Miya, G. Lecointre, G. Ortí, Phylogenetic classification of bony fishes, BMC Evol. Biol. 17 (2017) 162 https://doi.org/10.1186/s12862-017-0958-3.
[39] L.C. Hughes, G. Ortí, Y. Huang, Y. Sun, C.C. Baldwin, A.W. Thompson, D. Arcila, R. Betancur-R, C. Li, L. Becker, N. Bellora, X. Zhao, X. Li, M. Wang, C. Fang, B. Xie, Z. Zhou, H. Huang, S. Chen, B. Venkatesh, Q. Shi, Comprehensive phylogeny of ray-finned fishes (Actinopterygii) based on transcriptomic and genomic data, Proc. Natl. Acad. Sci. U.S.A. 115 (2018) 6249–6254 https://doi.org/10.1073/pnas.1719358115.
[40] D.J. Macqueen, I.A. Johnston, A well-constrained estimate for the timing of the salmonid whole genome duplication reveals major decoupling from species diversification, Proc. Biol. Sci. 281 (2014) 20132881https://doi.org/10.1098/rspb.2013.2881.
[41] S.M.K. Glasauer, S.C.F. Neuhauss, Whole-genome duplication in teleost fishes and its evolutionary consequences, Mol. Genet. Genom. 289 (2014) 1045–1060 https://doi.org/10.1007/s00438-014-0889-2.
[42] B. Venkatesh, A.P. Lee, V. Ravi, A.K. Maurya, M.M. Lian, J.B. Swann, Y. Ohta, M.F. Flajnik, Y. Sutoh, M. Kasahara, S. Hoon, V. Gangu, S.W. Roy, M. Irimia, V. Korzh, I. Kondrychyn, Z.W. Lim, B.H. Tay, S. Tohari, K.W. Kong, S. Ho, B. Lorente-Galdos, J. Quilez, T. Marques-Bonet, B.J. Raney, P.W. Ingham, A. Tay, L.D.W. Hillier, P. Minx, T. Boehm, R.K. Wilson, S. Brenner, W.C. Warren, Elephant shark genome provides unique insight into gnathostome evolution, Nature 50 (2014) 174–179 http://doi.org/10.1038/nature12826.
[43] M.D. Brazeau, M. Friedman, The origin and early phylogenetic history of jawed vertebrates, Nature 520 (2015) 490–497 https://doi.org/10.1038/nature14438.
[44] T. Qiao, B. King, J.A. Long, P.E. Ahlberg, M. Zhu, Early gnathostome phylogeny revisited: multiple method consensus, PLoS One 11 (2016) e0163157https://doi.org/10.1371/journal.pone.0163157.
[45] M. Zhu, W. Zhao, L. Jia, J. Lu, T. Qiao, Q. Qu, The oldest articulated osteichthyan reveals mosaic gnathostome characters, Nature 458 (2009) 469–474 https://doi.org/10.1038/nature07855.
[46] M. Nikaido, H. Noguchi, H. Nishihara, A. Toyoda, Y. Suzuki, R. Kajitani, H. Suzuki, M. Okuno, M. Aibara, B.P. Ngatunga, S.I. Mzighani, H.W.J. Kalombo, K.W.A. Masengi, J. Tuda, S. Nogami, R. Maeda, M. Iwata, Y. Abe, K. Fujimura, M. Okabe, T. Amano, A. Maeno, T. Shiroishi, T. Itoh, S. Sugano, Y. Kohara, A. Fujiyama, N. Okada, Coelacanth genomes reveal signatures for evolutionary transition from water to land, Genome Res. 23 (2013) 1740–1748 https://doi.org/10.1101/gr.158105.113.
[47] L. Cavin, G. Guinot, 2014. Coelacanths as “almost living fossils”, Front. Ecol. Evol. 13 (2014) 1–5 https://doi.org/10.3389/fevo.2014.00049.
[48] H.X. Li, X.J. Lu, C.H. Li, J. Chen, Molecular characterization and functional analysis of two distinct liver-expressed antimicrobial peptide 2 (LEAP-2) genes in large yellow croaker (*Larimichthys crocea*), Fish Shellfish Immunol. 38 (2014) 330–339 https://doi.org/10.1016/j.fsi.2014.04.004.
[49] T. Liang, W. Ji, G.R. Zhang, K.J. Wei, K. Feng, W.M. Wang, G.W. Zou, Molecular cloning and expression analysis of liver-expressed antimicrobial peptide 1 (LEAP-1) and LEAP-2 genes in the blunt snout bream (*Megalobrama amblycephala*), Fish

Shellfish Immunol. 35 (2013) 553–563 https://doi.org/10.1016/j.fsi.2013.05.021.
[50] E. Gisbert, Y.K. Nam, Early ontogeny in the Siberian sturgeon, in: P. Williot, G. Nonnotte, D. Vizziano-Cantonnet, M. Chebanov (Eds.), The Siberian Sturgeon (*Acipenser baerii*, Brandt, 1869), Springer International Publishing AG., Cham, 2018, pp. 131–157 https://doi.org/10.1007/978-3-319-61664-3_8.
[51] E.J. Kim, C.H. Park, Y.K. Nam, Effects of incubation temperature on the embryonic viability and hatching time in Russian sturgeon (*Acipenser gueldenstaedtii*), Fish. Aquat. Sci. 21 (2018) 1–8 https://doi.org/10.1186/s41240-018-0101-4.
[52] E. Gisbert, M. Solovyev, Behaviour of early life stages in the Siberian sturgeon, in: P. Williot, G. Nonnotte, D. Vizziano-Cantonnet, M. Chebanov (Eds.), The Siberian Sturgeon (*Acipenser baerii*, Brandt, 1869), Springer International Publishing AG., Cham, 2018, pp. 159–172 https://doi.org/10.1007/978-3-319-61664-3_9.
[53] E. Gisbert, P. Williot P, F. Castelló-Orvay, Behavioural modifications in the early life stages of Siberian sturgeon (*Acipenser baerii*, Brandt), J. Appl. Ichthyol. 15 (1999) 237–242 https://doi.org/10.1111/j.1439-0426.1999.tb00242.x.
[54] G. Ren, W.Y. Shen, W.F. Li, Y.R. Zhu, Molecular characterization and expression pattern of a liver-expressed antimicrobial peptide 2 (LEAP-2) gene in yellow catfish (*Pelteobagrus fulvidraco*), J. Aquac. Res. Dev. 299 (2014) 1000229https://doi.org/10.4172/2155-9546.1000229.
[55] M.M. Guarna, R. Coulson, E. Rubinchik, Anti-inflammatory activity of cationic peptides: application to the treatment of acne vulgaris, FEMS Microbiol. Lett. 257 (2006) 1–6, https://doi.org/10.1111/j.1574-6968.2006.00156.x.
[56] L.-H. Li, T.-C. Ju, C.-Y. Hsieh, W.-C. Dong, W.-T. Chen, K.-F. Hua, W.J. Chen, A synthetic cationic antimicrobial peptide inhibits inflammatory response and the NLRP3 inflammasome by neutralizing LPS and ATP, PLoS One 12 (2017) e0182057https://doi.org/10.1371/journal.pone.0182057.
[57] O. Al-Massadi, T. Müller, M. Tschöp, C. Diéguez, R. Nogueiras, Ghrelin and LEAP-2: rivals in energy metabolism, Trends Pharmacol. Sci. 39 (2018) 685–694 https://doi.org/10.1016/j.tips.2018.06.004.
[58] X. Ge, H. Yang, M.A. Bednarek, H. Galon-Tilleman, P. Chen, M. Chen, J.S. Lichtman, Y. Wang, O. Dalmas, Y. Yin, H. Tian, L. Jermutus, J. Grimsby, C.M. Rondinone, A. Konkar, D.D. Kaplan, LEAP2 is an endogenous antagonist of the ghrelin receptor, Cell Metabol. 27 (2018) 461–469 https://doi.org/10.1016/j.cmet.2017.10.016.